

Received July 17, 2020, accepted August 23, 2020, date of publication August 25, 2020, date of current version September 3, 2020.

Digital Object Identifier 10.1109/ACCESS.2020.3019475

Research on the Folding Spring Triboelectric Nanogenerator for Rock Climbing Trajectory and Time Monitoring

JUN ZHANG¹, CHUAN WU², AND QING ZHOU²

¹School of Sports Economics and Management, Hubei University of Economics, Wuhan 430205, China

²School of Mechanical and Electronic Information, China University of Geosciences at Wuhan, Wuhan 430074, China

Corresponding authors: Jun Zhang (smilezjun@163.com) and Chuan Wu (wuchuan@cug.edu.cn)

This work was supported by the China Postdoctoral Science Foundation under Grant 2019M650237.

ABSTRACT The monitoring data of climbing trajectory and climbing time in rock climbing training are the basis for coaches to select athletes and formulate the next training plans. This article proposes a folding spring triboelectric nanogenerator that can be used for trajectory training and time training in rock climbing training. The folding spring triboelectric nanogenerator, made of PMMA (polymethyl methacrylate), Kapton, PTFE (Polytetrafluoroethylene), Cu (copper) and PLA (polylactic acid), realizes the detection functions based on the voltage pulse generated by the vertical friction between each two adjacent friction layers, and then the width of the output voltage pulse is the training time and the envelope of the space area formed by all the contacted folding spring triboelectric nanogenerator is the climbing trajectory. Test results show that the output voltage amplitude are between 7.5 V and 10.8 V, the output current will drop sharply from 24.5×10^{-7} A when the load resistance exceeds 47k ohms, the time interval between two consecutive uses should be greater than 0.2 s, and the maximum output power is 163.6×10^{-8} W when a 4.7×10^6 ohm load resistance is connected in series, which shows a strong signal-to-noise ratio and anti-interference ability. In addition, the trajectory training and the time training tests results show that the folding spring triboelectric nanogenerator can be used for real-time monitoring in rock climbing training, but it needs to be pressed twice in succession when used for time training limited by the structural and principle.


INDEX TERMS Triboelectric nanogenerator, self-powered sensor, rock climbing, climbing trajectory.

I. INTRODUCTION

Rock climbing is a sport that relies on hands and feet to climb rock points on natural or artificial climbing walls to achieve the purpose of upward climbing [1], and its basic training contents include trajectory training and time training. Trajectory training means the routes from the bottom to the top of the climbing wall formed by the athletes when climbing, and it can test the ability of athletes because different routes represent different difficulties[2]. Time training means the time in which athletes rely on their fingers to grab a rock point and hang their entire body, and it can also test the ability of athletes because the longer the suspension time, the stronger the athletes [3], [4]. Data of trajectory training and time training are the basis for coaches to select athletes and formulate the

next training plans, but there are no professional measuring instruments at present. The data recording methods still relies on manual recording after visual observation, which means high labor intensity, high error and low efficiency. Therefore, there is an urgent need to develop professional instruments to meet the requirements of rock climbing trajectory training and time training.

The triboelectric nanogenerator was proposed by Z. L. Wang in 2012 [5], and the current research focus include energy harvesting [6]–[8], sensors [9]–[11], new materials [12]–[14], and so on. Especially in the filed of sensors, the triboelectric nanogenerator have been widely used in wearable devices [15], [16], gas detection [17], [18], light detection [19], environmental monitoring [20], [21], geological exploration [22], [23], wind speed monitoring [24], [25], robot sensing [26], [27], oil and gas resources [28], and so on. Some scholars have also conducted some research

The associate editor coordinating the review of this manuscript and approving it for publication was Gongbo Zhou .

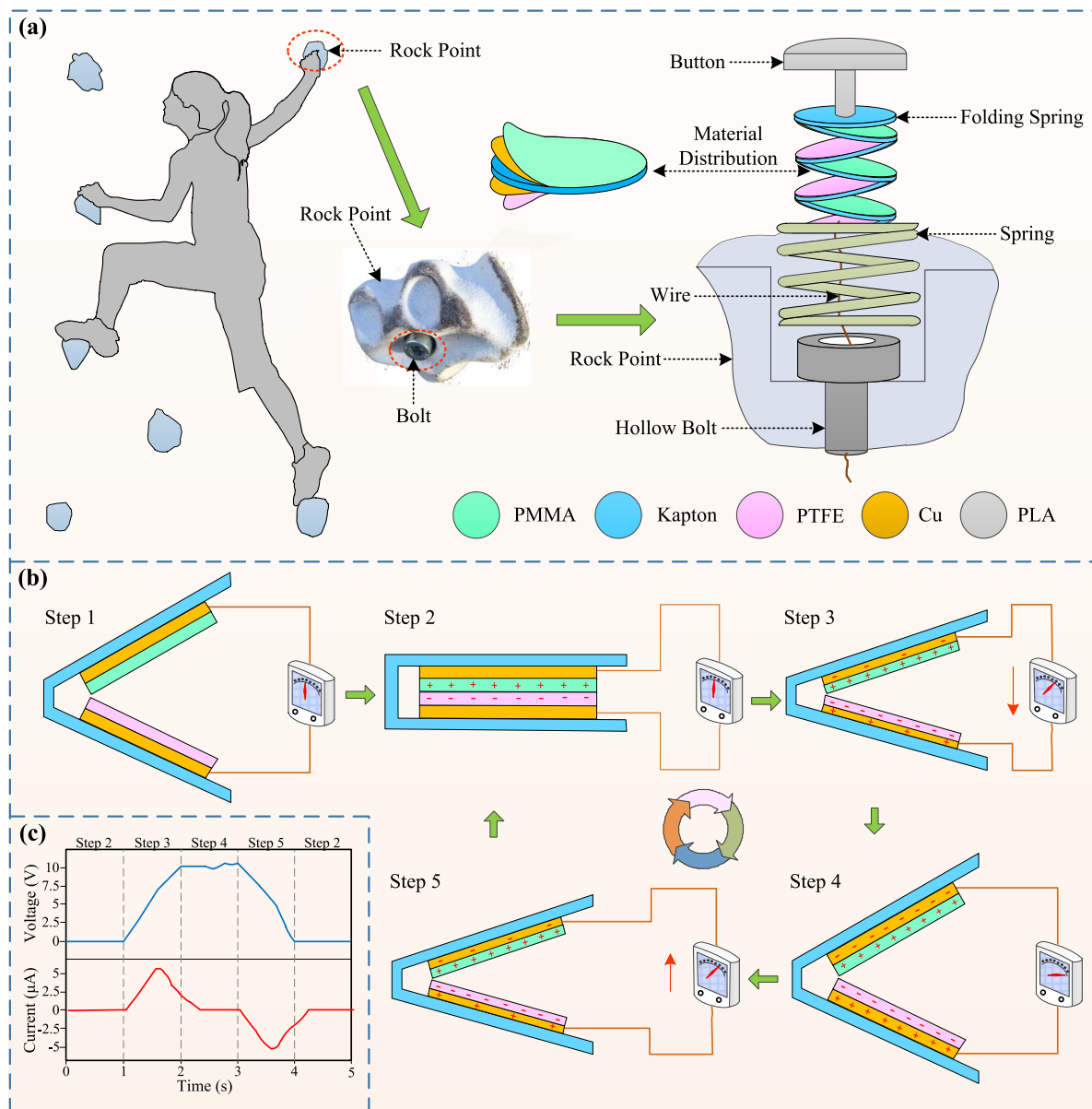


FIGURE 1. Schematic diagram of the FS-TENG working principle. (a) Composition of the FS-TENG; (b) Schematic diagram of working process of the FS-TENG; (c) Theoretical output signal of the FS-TENG.

in the application of sports, such as human body energy collection [29], [30], walking pattern recognition [31], gait detection [32], and sports detection [33]. Because the sensors that developed based on the triboelectric nanogenerator have the function of self-powered, it is particularly suitable for the rock climbing training. Therefore, this article proposes a folding spring triboelectric nanogenerator (or FS-TENG, for short) that can be used for trajectory training and time training in rock climbing, so as to provide the necessary measurement data for coaches.

II. MANUFACTURING AND WORKING PRINCIPLE

As shown in figure 1(a), the rock points fixed on the indoor climbing wall by bolts are artificially manufactured, so our design idea is to expand the size of the bolt mounting hole to

install the FS-TENG, and then replace the bolt with hollow bolt to make the signal wires to pass through. As one of the main components of the FS-TENG, the folding spring, with a size of $\varphi 25 \times 20$ mm, is made of a 0.05 mm thick Kapton (PY11YG, Lingmei Co., LTD, Dongguan, China) to ensure elastic deformation, and any two adjacent surfaces of the folding spring are pasted with different nanomaterials to form the friction layers. One of the friction layers is made of PTFE (CTF30, Bench Co., LTD., Suzhou, Jiangsu, China) with a thickness of 0.03 mm, and the other is PMMA (0703, Chuangyou Co., LTD, Suzhou, China) with a thickness of 0.2 mm. Cu (C1100, ZYTLCL Co., LTD., Dongguan, Guangdong, China) with a thickness of 0.05 mm is used as electrode layer under both friction layers.

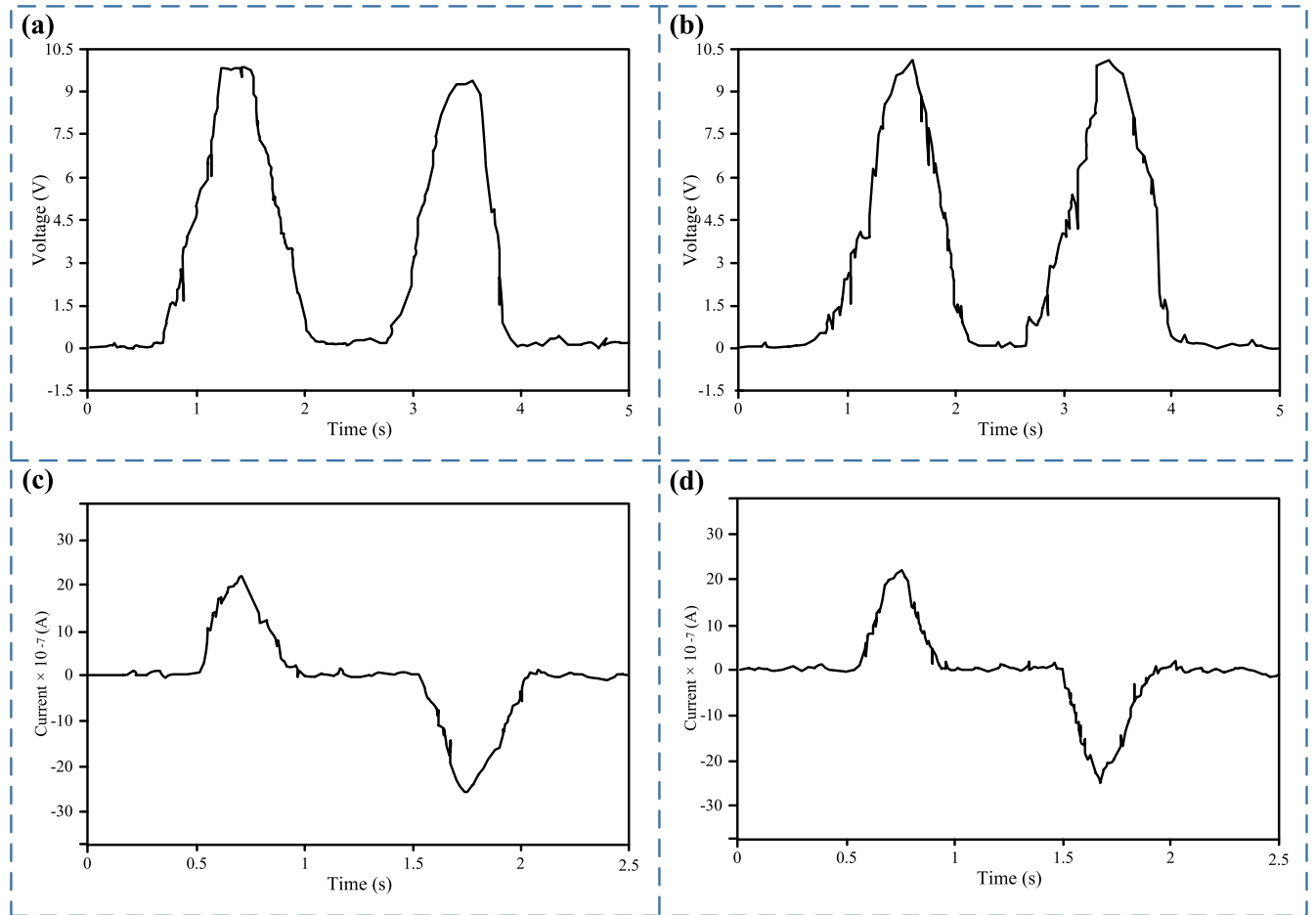


FIGURE 2. Output signal of the FS-TENG. (a) Output voltage of the FS-TENG pressed twice by hands; (b) Output voltage of the FS-TENG pressed twice by feet; (c) Output current of the FS-TENG pressed once by hands (with a 4.7×10^4 k resistance in series); (d) Output current of the FS-TENG pressed once by feet (with a 4.7×10^4 k resistance in series).

The folding spring, embedded in the spring, fixed in the rock point together with the hollow bolt, and all the same friction layers in the folding spring are connected by wires. The folding spring and the spring will be deformed together when the FS-TENG is pressed by athletes, thus causing frictional electrification on any two adjacent surfaces of the folding spring. Subsequently, the contacted surfaces will gradually separate due to the restoring force of the spring when the pressing force disappears, thus generating charges transfer, so the detection function of whether the athletes pressure the rock point can be achieved by further analyzing the rule of transferred charges. Then the envelope of the formed area in the software is the training trajectory when all the pressed FS-TENG are spatially located to the corresponding coordinates in the software, and the duration of the pressing signal of the single FS-TENG is the training time.

As shown in figure 1(b), the working principle of the FS-TENG can be further explained by taking any adjacent two surfaces of the folding spring as an example. Step 1 is the initial state where there is no contact between the two

surfaces. Step 2 is the state where the two surfaces are in contact with each other under the pressure of the athletes, and the friction layer with PMMA is positively charged while the PTFE is negatively charged because PMMA is more likely to lose electrons. Step 3 is the state where the two surfaces are gradually separated under the spring restoring force, and a short-circuit current is generated and the open-circuit voltage gradually expands with the separation distance expands. Step 4 is the state where the two surfaces are separated to the maximum distance, and the open-circuit voltage thus reaches the maximum value. Step 5 is the state where the two surfaces are gradually approach each other when the athletes presses again, and a reverse short-circuit current is generated and the open-circuit voltage gradually decreases with the separation distance decreases. Then the open-circuit voltage is reduced to zero when finally returning to Step 2. In the above steps, the theoretical output voltage and current signal are shown in figure 1(c). As a voltage pulse signal will be generated no matter the FS-TENG is pressed for the first time or more than the second time, a single voltage pulse is selected as the detection signal in this article.

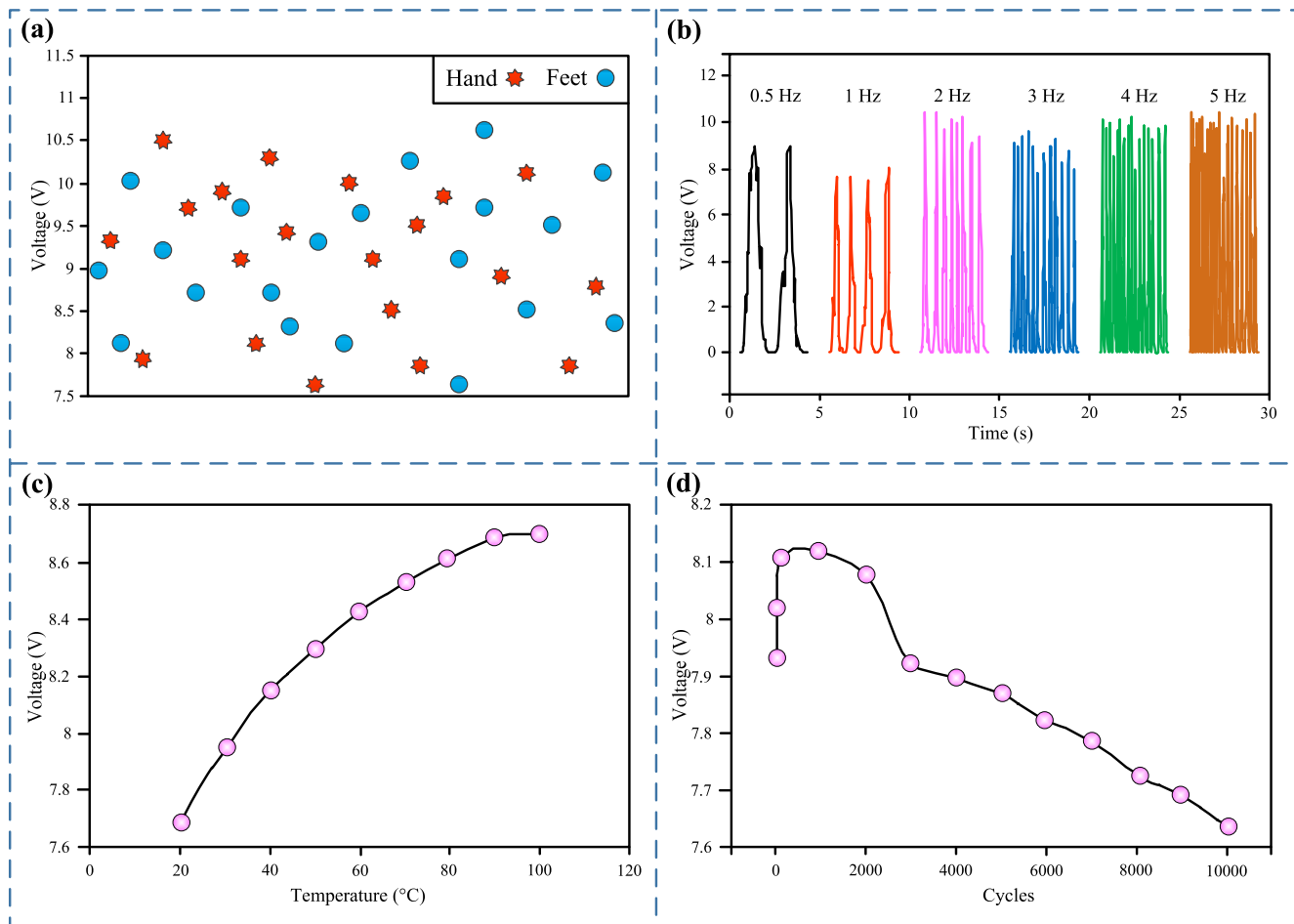


FIGURE 3. Test results of the FS-TENG output signal. (a) Scatter diagram of the FS-TENG output voltage amplitude; (b) Output voltage of the FS-TENG in different contact frequencies; (c) Output voltage of the FS-TENG in different temperatures; (d) Output voltage of the FS-TENG in different cycles.

III. TESTS

Tests are divided into two parts, one is to test the output performance of the FS-TENG, and the other is to test the functions of trajectory training and time training, which are introduced separately as follows.

Figure 2 shows the output signal of the FS-TENG, and we can obtain that the FS-TENG will output a voltage or current pulse signal no matter it is pressed by hands or feet, so the contact detection function can be realized by connecting the output signal wire to the pulse counting pin of any MCU (Microprogrammed Control Unit). In addition, the reason why the waveform of the hands are smoother than the feet is that there are strong jitter when pressed by feet.

Figure 3 shows the test results of the FS-TENG output signal, and we can obtain the following conclusions. (1) The number of output voltage tests are 1000, in which hands and feet account for half, and parts of the test data are shown in figure 3(a). As shown in figure 3(a), the output voltage distribution are irregular, but the amplitude are concentrated between 7.5 V and 10.8 V, which are much larger than the noise signal and shows a strong signal-to-noise. (2) As shown in figure 3(b), the FS-TENG can still work normally at a

working frequency of 5 Hz, which indicates that the time interval between two consecutive uses should be greater than 0.2 s. (3) As shown in figure 3(c), the output voltage will gradually increase from 7.65 V to 8.7 V as the ambient temperature rises to 100 degrees Celsius. The larger the signal amplitude, the easier to be detected, so the higher the temperature within 100 degrees Celsius, the stronger the signal-to-noise ratio and anti-interference ability of the FS-TENG. (4) We did 10000 tests to test the reliability of the FS-TENG, and each test is the averaged for 10 seconds measurement. As shown in figure 3(d), the output voltage increases to 8.12 V and then gradually decreases to 7.62 V as the number of tests increases, but it still shows a high signal-to-noise ratio even if the output voltage reduce to 7.62 V, which shows a high reliability. However, the output performance will be affected by long-term wear, so wear-resistant materials or metal materials will be selected as friction layers in the next study to improve the long-term stability.

Figure 4 shows the test results of the FS-TENG power generation performance, and we can obtain the following conclusions. (1) As shown in figure 4(a), the output current is different because the pressure of fingers, hands and feet

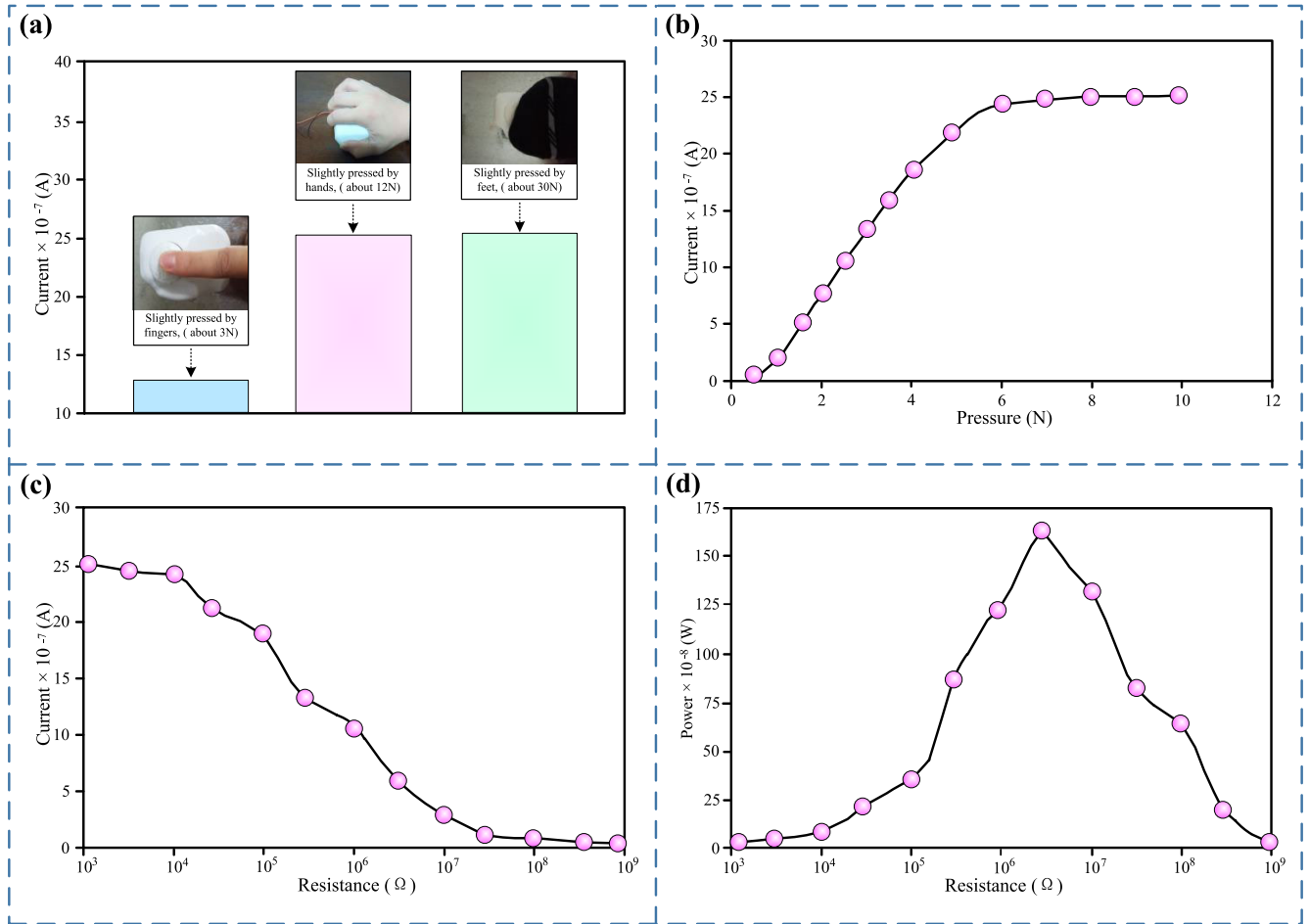


FIGURE 4. Test results of the FS-TENG power generation. (a) Output current of the FS-TENG pressed by hands or feet; (b) Output current of the FS-TENG in different pressures when a 10^3 ohm resistances is connected in series; (c) Output current of the FS-TENG in different load resistances when the pressure is greater than 10 N; (d) Output power of the FS-TENG in different load resistances when the pressure is greater than 10 N.

are different, so we tested the output current under different pressures, and the results are shown in figure 4(b). As shown in figure 4(b), the output current gradually increases with the increase of pressure, and it will reach a maximum value when the pressure exceeds 8 N. Because the climbing pressures in actual rock climbing are much greater than 8 N, the FS-TENG will output the maximum current no matter it is pressed by hands or feet. (2) As shown in figure 4(c), the output current gradually decreases with the increase of resistance, and it will drop sharply from 24.5×10^{-7} A when the resistance exceeds 47k ohms, so a resistance less than 47k ohms can be connected in series to obtain a larger output signal when the output current is selected as the detection signal. (3) As shown in figure 4(d), the FS-TENG can output a maximum power of 163.6×10^{-8} W when the load resistance is about 4.7×10^6 ohms, so a resistance about 4.7×10^6 ohm can be connected in series to obtain a larger output power when the FS-TENG is used as a power source.

Figure 5 shows the test results of the FS-TENG used for trajectory training and time training, and we can obtain

the following conclusions. (1) As shown in figure 5(a), the FS-TENG is installed on the rock point, and its output signal are input into the software after being processed by the electrometer (6514, Keithley Co., LTD., Solon, America) and the MCU (USB5632, ART Technology Co., LTD., Beijing, China) in turn. As shown in figure 5(b), each rock point with a specific spatial coordinate on the climbing wall can be mapped to the indicator light at the corresponding coordinate in the software by programming in LabView language. The indicator light at the corresponding coordinate in the software will be lit red when the athletes contact the rock point, and then the envelope of the area formed by all red indicators is the climbing trajectory. (2) As show in figure 5(c), figure 5(d), figure 1(b) and figure 1(c), the training time of the athletes is the time corresponding to Step 2 which shown in figure 5(c) or figure 5(d). Because the time for Step 2 cannot be recognized in figure 5(c) while it can be measured by counting the output voltage pulse width in figure 5(d), the athletes must press the FS-TENG twice in a row if used for time training detection.

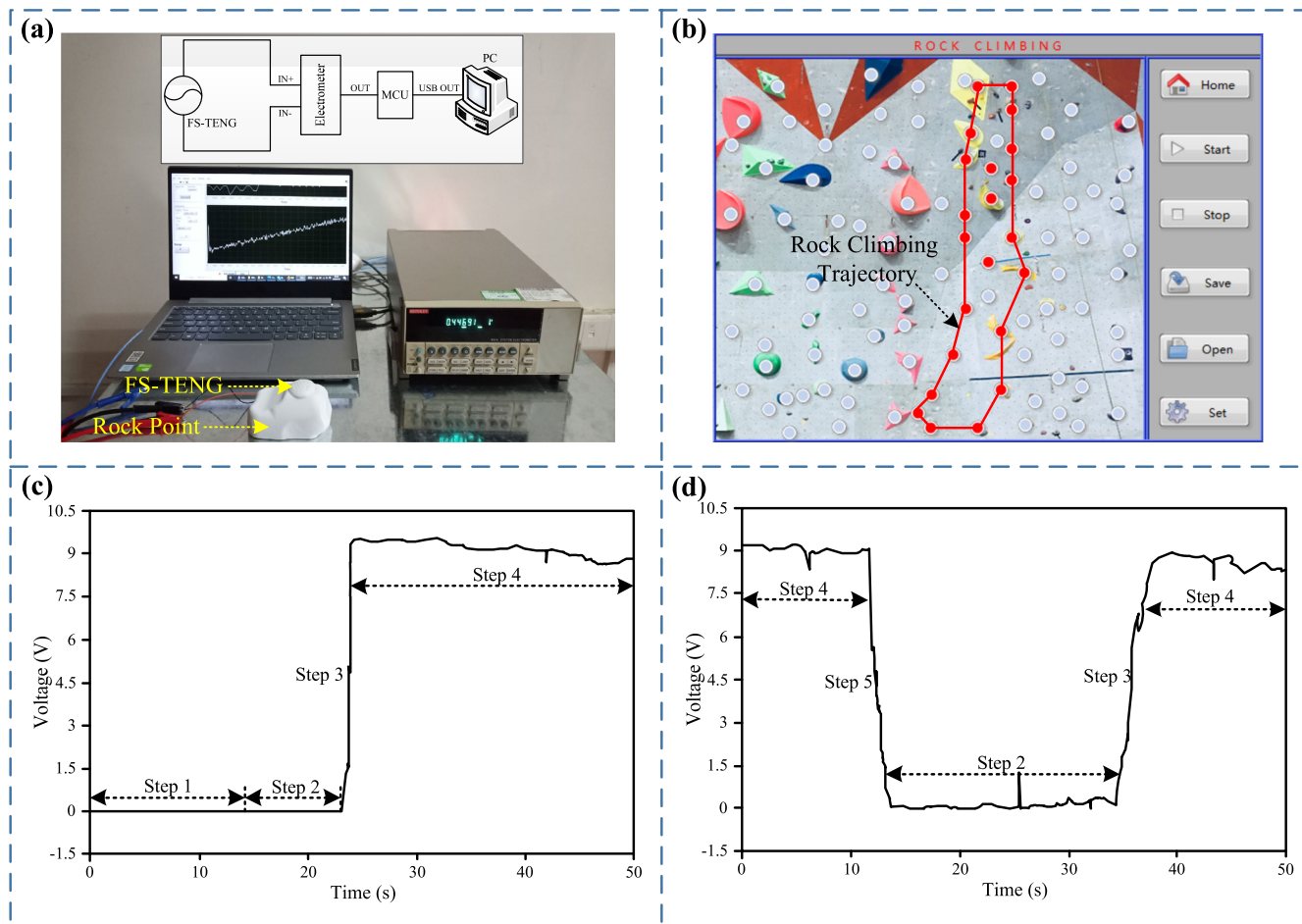


FIGURE 5. Test results of the FS-TENG used for trajectory training and time training. (a) A picture of the test devices; (b) Test result of the trajectory training shown in software; (c) Output voltage curve of the time training when the FS-TENG is pressed for the first time; (d) Output voltage curve of the time training when the FS-TENG is pressed more than the second time.

IV. CONCLUSION AND DISCUSSIONS

The FS-TENG can meet the needs of trajectory training and time training in rock climbing. The width of the output voltage pulse is the training time, and the envelope of the space area formed by all the contacted FS-TENG is the climbing trajectory. Test results show that the output voltage amplitude are between 7.5 V and 10.8 V, the output current signal are larger than 24.5×10^{-7} A when the series resistance is less than 47k ohms, the interval between two consecutive uses should be greater than 0.2 s, and has a strong anti-interference ability and reliability. In addition, the FS-TENG can output a maximum power of 163.6×10^{-8} W when the load resistance is about 4.7×10^6 ohms, so a resistance about 4.7×10^6 ohm can be connected in series to obtain a larger output power when used as a power source.

But there are still two aspects that need to be further improved. One is that the bolt mounting holes of the rock point need to be enlarged to install the FS-TENG, so the next step is to change the structure into a bolt shape to replace the original one for installation, thereby avoiding changing the rock point. The other is that the athletes need to press the FS-TENG twice in a row when used for time training,

so the next step is to change the triggering mode to realize the function that the friction layer of the FS-TENG contact twice when pressed once, thereby simplifying the operation.

REFERENCES

- [1] D. Aras and A. W. Ewert, “The effects of eight weeks sport rock climbing training on anxiety,” *Acta Medica Mediterranea*, vol. 32, no. 1, pp. 223–230, 2016.
- [2] A. I. Grushko and S. V. Leonov, “The usage of eye-tracking technologies in rock-climbing,” *Procedia-Social Behav. Sci.*, vol. 146, pp. 169–174, Aug. 2014.
- [3] J. Baláš, M. Panáčková, J. Kodejška, J. D. Cochrane, and J. A. Martin, “The role of arm position during finger flexor strength measurement in sport climbers,” *Int. J. Perform. Anal. Sport*, vol. 14, no. 2, pp. 345–354, Aug. 2014.
- [4] M. Ozimek, R. Staszkievicz, R. Rokowski, and A. Stanula, “Analysis of tests evaluating sport Climbers’ strength and isometric endurance,” *J. Hum. Kinetics*, vol. 53, no. 1, pp. 249–260, Dec. 2016.
- [5] F.-R. Fan, Z.-Q. Tian, and Z. Lin Wang, “Flexible triboelectric generator,” *Nano Energy*, vol. 1, no. 2, pp. 328–334, Mar. 2012.
- [6] Z. L. Wang, T. Jiang, and L. Xu, “Toward the blue energy dream by triboelectric nanogenerator networks,” *Nano Energy*, vol. 39, pp. 9–23, Sep. 2017.
- [7] H. B. Lin, M. H. He, Q. S. Jing, W. F. Yang, S. T. Wang, Y. Liu, Y. L. Zhang, N. Li, Y. Ma, and L. Wang, “Angle-shaped triboelectric nanogenerator for harvesting environmental wind energy,” *Nano Energy*, vol. 56, pp. 269–276, Feb. 2019.

- [8] X. Pu, M. Liu, X. Chen, J. Sun, C. Du, Y. Zhang, J. Zhai, W. Hu, and Z. L. Wang, "Ultrastretchable, transparent triboelectric nanogenerator as electronic skin for biomechanical energy harvesting and tactile sensing," *Sci. Adv.*, vol. 3, no. 5, May 2017, Art. no. e1700015.
- [9] D. Heo, T. Kim, H. Yong, K. T. Yoo, and S. Lee, "Sustainable oscillating triboelectric nanogenerator for omnidirectional self-powered impact sensor," *Nano Energy*, vol. 50, pp. 1–8, Aug. 2018.
- [10] C. Qian, L. Li, M. Gao, H. Yang, Z. Cai, B. Chen, Z. Xiang, Z. Zhang, and Y. Song, "All-printed 3D hierarchically structured cellulose aerogel based triboelectric nanogenerator for multi-functional sensors," *Nano Energy*, vol. 63, Sep. 2019, Art. no. 103885.
- [11] J. Luo, Z. Wang, L. Xu, A. C. Wang, K. Han, T. Jiang, Q. Lai, Y. Bai, W. Tang, F. R. Fan, and Z. L. Wang, "Flexible and durable wood-based triboelectric nanogenerators for self-powered sensing in athletic big data analytics," *Nature Commun.*, vol. 10, no. 1, pp. 1–9, Dec. 2019.
- [12] S. Hajra, M. Sahu, B. K. Panigrahi, and R. N. P. Choudhary, "Excitation performance of $\text{Ba}_{0.8}\text{Mg}_{0.2}(\text{Zr}_{0.1}\text{Ti}_{0.8}\text{Ce}_{0.1})\text{O}_3$ materials in an electrical field," *Pramana*, vol. 93, no. 3, p. 48, 2019.
- [13] G. Khandelwal, N. P. M. J. Raj, and S. Kim, "Zeolitic imidazole framework: Metal–organic framework subfamily members for triboelectric nanogenerators," *Adv. Funct. Mater.*, vol. 30, no. 12, Mar. 2020, Art. no. 1910162.
- [14] G. Khandelwal, A. Chandrasekhar, N. P. M. J. Raj, and S. Kim, "Metal–organic framework: A novel material for triboelectric nanogenerator–based self-powered sensors and systems," *Adv. Energy Mater.*, vol. 9, no. 14, p. 1803581, 2019.
- [15] A. R. Mule, B. Dudem, H. Patnam, S. A. Graham, and J. S. Yu, "Wearable single-electrode-mode triboelectric nanogenerator via conductive polymer-coated textiles for self-power electronics," *ACS Sustain. Chem. Eng.*, vol. 7, no. 19, pp. 16450–16458, Oct. 2019.
- [16] J. Xiong, P. Cui, X. Chen, J. Wang, K. Parida, M.-F. Lin, and P. S. Lee, "Skin-touch-actuated textile-based triboelectric nanogenerator with black phosphorus for durable biomechanical energy harvesting," *Nature Commun.*, vol. 9, no. 1, pp. 1–9, Dec. 2018.
- [17] Y. Su, G. Xie, H. Tai, S. Li, B. Yang, S. Wang, Q. Zhang, H. Du, H. Zhang, X. Du, and Y. Jiang, "Self-powered room temperature NO_2 detection driven by triboelectric nanogenerator under UV illumination," *Nano Energy*, vol. 47, pp. 316–324, May 2018.
- [18] J. Chang, H. Meng, C. Li, J. Gao, S. Chen, Q. Hu, H. Li, and L. Feng, "A wearable toxic gas-monitoring device based on triboelectric nanogenerator for self-powered aniline early warning," *Adv. Mater. Technol.*, vol. 5, no. 5, May 2020, Art. no. 1901087.
- [19] L. Han, M. Peng, Z. Wen, Y. Liu, Y. Zhang, Q. Zhu, H. Lei, S. Liu, L. Zheng, X. Sun, and H. Li, "Self-driven photodetection based on impedance matching effect between a triboelectric nanogenerator and a MoS_2 nanosheets photodetector," *Nano Energy*, vol. 59, pp. 492–499, May 2019.
- [20] Z. Zhou, X. Li, Y. Wu, H. Zhang, Z. Lin, K. Meng, Z. Lin, Q. He, C. Sun, J. Yang, and Z. L. Wang, "Wireless self-powered sensor networks driven by triboelectric nanogenerator for *in-situ* real time survey of environmental monitoring," *Nano Energy*, vol. 53, pp. 501–507, Nov. 2018.
- [21] Q. Shi, H. Wang, H. Wu, and C. Lee, "Self-powered triboelectric nanogenerator buoy ball for applications ranging from environment monitoring to water wave energy farm," *Nano Energy*, vol. 40, pp. 203–213, Oct. 2017.
- [22] C. Wu, H. Huang, R. Li, and C. Fan, "Research on the potential of spherical triboelectric nanogenerator for collecting vibration energy and measuring vibration," *Sensors*, vol. 20, no. 4, p. 1063, Feb. 2020.
- [23] C. Wu, C. Fan, and G. Wen, "Self-powered speed sensor for turbodrills based on triboelectric nanogenerator," *Sensors*, vol. 19, no. 22, p. 4889, Nov. 2019.
- [24] J. Wang, W. Ding, L. Pan, C. Wu, H. Yu, L. Yang, R. Liao, and Z. L. Wang, "Self-powered wind sensor system for detecting wind speed and direction based on a triboelectric nanogenerator," *ACS Nano*, vol. 12, no. 4, pp. 3954–3963, Apr. 2018.
- [25] D. Kim, I.-W. Tcho, and Y.-K. Choi, "Triboelectric nanogenerator based on rolling motion of beads for harvesting wind energy as active wind speed sensor," *Nano Energy*, vol. 52, pp. 256–263, Oct. 2018.
- [26] Z. Yuan, G. Shen, C. Pan, and Z. L. Wang, "Flexible sliding sensor for simultaneous monitoring deformation and displacement on a robotic hand/arm," *Nano Energy*, vol. 73, Jul. 2020, Art. no. 104764.
- [27] X. Chen, T. Jiang, Y. Yao, L. Xu, Z. Zhao, and Z. L. Wang, "Stimulating acrylic elastomers by a triboelectric nanogenerator–toward self-powered electronic skin and artificial muscle," *Adv. Funct. Mater.*, vol. 26, no. 27, pp. 4906–4913, Jul. 2016.
- [28] C. Fan, C. Wu, and G. Wen, "Development of gas–liquid two-phase flow pattern sensor of coalbed methane based on the principle of triboelectric nanogenerator," *Nanotechnology*, vol. 31, no. 19, May 2020, Art. no. 195501.
- [29] Z. Tian, J. He, X. Chen, T. Wen, C. Zhai, Z. Zhang, J. Cho, X. Chou, and C. Xue, "Core–shell coaxially structured triboelectric nanogenerator for energy harvesting and motion sensing," *RSC Adv.*, vol. 8, no. 6, pp. 2950–2957, 2018.
- [30] K. Xia, Z. Zhu, H. Zhang, C. Du, Z. Xu, and R. Wang, "Painting a high-output triboelectric nanogenerator on paper for harvesting energy from human body motion," *Nano Energy*, vol. 50, pp. 571–580, Aug. 2018.
- [31] M. Zhu, Q. Shi, T. He, Z. Yi, Y. Ma, B. Yang, T. Chen, and C. Lee, "Self-powered and self-functional cotton sock using piezoelectric and triboelectric hybrid mechanism for healthcare and sports monitoring," *ACS Nano*, vol. 13, no. 2, pp. 1940–1952, Feb. 2019.
- [32] Z. Lin, Z. Wu, B. Zhang, Y.-C. Wang, H. Guo, G. Liu, C. Chen, Y. Chen, J. Yang, and Z. L. Wang, "A triboelectric nanogenerator-based smart insole for multifunctional gait monitoring," *Adv. Mater. Technol.*, vol. 4, no. 2, Feb. 2019, Art. no. 1800360.
- [33] Y. Xi, J. Hua, and Y. Shi, "Noncontact triboelectric nanogenerator for human motion monitoring and energy harvesting," *Nano Energy*, vol. 69, Mar. 2020, Art. no. 104390.



JUN ZHANG was born in Xiangyang, Hubei, China, in 1989. She received the B.S. degree in social sports guidance and management from the China University of Geosciences at Wuhan, in 2012, and the M.S. degree in sports humanities and sociology from the Huazhong University of Science and Technology, in 2015.

From 2015 to 2020, she was a Lecturer with the School of Sports Economics and Management, Hubei University of Economics, Wuhan, China.

Her research interests include rock climbing and equipment, orienteering, and sports venue management.



CHUAN WU was born in Handan, Hebei, China, in 1986. He received the B.S. degree in mechanical design, manufacturing, and automation and the Ph.D. degree in geological engineering from the China University of Geosciences at Wuhan, Wuhan, China, in 2011 and 2016, respectively.

From October 2016 to February 2017, he was a Research Assistant with the Biomedical Robot Laboratory, The Chinese University of Hong Kong, Hong Kong. From March 2017 to 2020,

he was an Associate Professor with the School of Mechanical and Electronic Information, China University of Geosciences at Wuhan. His research interests include self-powered sensors, physical sensors, mechatronics equipment, and the applications in oil and gas resources and industrial automation.



QING ZHOU was born in Hengyang, Hunan, China, in 1997. He received the B.S. degree in electronic information engineering from the Hunan University of Science and Technology, in 2019. He is currently pursuing the M.S. degree in mechanical engineering with the China University of Geosciences at Wuhan.

His research interests include self-powered sensors, physical sensors, mechatronics equipment, and the applications in oil and gas resources and industrial automation.

...